

# Mechanistic Studies on the Wolff Rearrangement: The Chemistry and Spectroscopy of Some $\alpha$ -Ketocarbenes<sup>†</sup>

Robert J. McMahon, Orville L. Chapman,\* Richard A. Hayes, Thomas C. Hess, and Hans-Peter Krimmer

Contribution from the Department of Chemistry and Biochemistry, University of California, Los Angeles, Los Angeles, California 90024. Received March 15, 1985

**Abstract:** Photochemical extrusion of dinitrogen from diazo ketones **1-4** matrix isolated in argon at 10–15 K produces  $\alpha$ -ketocarbenes **5, 6,** and **8**. UV-vis, infrared, and electron spin resonance spectroscopy identify the  $\alpha$ -ketocarbenes, which are further characterized by trapping with carbon monoxide and dioxygen. Excitation ( $T_0-T_1$ ) of the  $\alpha$ -ketocarbenes leads to rapid ring contraction of **5**→**9** and slow ring contraction of **6**→**10** and **8**→**12**. This trend parallels the increasing degree of strain in the product ketenes. Shorter wavelength irradiation causes rapid ring contraction of **6**→**10** and **8**→**12**. The stepwise Wolff rearrangement of **1-4** proceeds through an  $\alpha$ -ketocarbene. Ring contraction occurs in a singlet excited state ( $S''$ ) formed upon photolysis of the primary product  $\alpha$ -ketocarbene ( $T_0$ ).

The chemistry of  $\alpha$ -diazo ketones is important in modern science and technology. Recent syntheses of perhydroazulene sesquiterpenes and monoterpene cyclopentanoid natural products utilize ketocarbenes derived from diazo ketones as key intermediates.<sup>1</sup> The Arndt-Eistert sequence employs the Wolff rearrangement of an  $\alpha$ -diazoketone to a ketene in the one-carbon homologation of carboxylic acids.<sup>2</sup> Ring contraction of cyclic diazo ketones represents a general method for the preparation of highly strained small-ring compounds.<sup>3</sup> Finally, diazo ketone chemistry supports the photolithography industry in the United States.<sup>4</sup>

An important mechanistic question in the Wolff rearrangement centers on whether dinitrogen loss and 1,2-migration occur in a concerted manner, or whether the rearrangement is actually a two-step process, which first proceeds through an  $\alpha$ -ketocarbene intermediate (of either single or triplet spin multiplicity).<sup>5</sup> Two microsecond flash photolysis studies of diazo ketones failed to detect any species other than ketene.<sup>6,7</sup> CIDNP studies indicate that the photochemical rearrangement of diazoacetone is a concerted reaction. Although both singlet and triplet acetylmethylene are formed, neither species is on the reaction coordinate to Wolff rearrangement.<sup>8</sup> Conformational studies by Kaplan and co-workers suggest that concerted rearrangement occurs from the *s-Z* conformation of  $\alpha$ -diazoketones.<sup>9</sup> Product ratios observed in direct and triplet-sensitized photolysis of  $\alpha$ -diazocarbonyl compounds required Tomioka to postulate a concerted component occurring from the *s-Z* conformation and a nonconcerted component occurring from the *s-E* conformation.<sup>10</sup> This explanation accounts for the formation of Wolff rearrangement products during triplet-sensitized irradiation. Initially formed triplet can equilibrate with singlet ketocarbene, which undergoes Wolff rearrangement. Other ketocarbene rearrangements may also occur.

Ketocarbene-ketocarbene interconversion has been well-established from thermal and photochemical studies of unsymmetrically substituted diazo ketones and from label scrambling in isotopically labeled diazo ketones.<sup>5,11-14</sup> Competing reactions of the singlet ketocarbene (interconversion with another singlet ketocarbene, intersystem crossing to the triplet, reaction with solvent or added trapping agent, and Wolff rearrangement) determine the degree of label scrambling.<sup>10,11</sup> Ketocarbene-ketocarbene interconversion must occur through an oxirene intermediate or an oxirene-like transition state.<sup>5,11</sup> Numerous theoretical calculations predict oxirene itself to be an energy minimum with a low barrier (2–8 kcal/mol) to rearrangement to ke-

tene.<sup>11,15,16</sup> (Singlet formylcarbene rearranges to ketene with no barrier.)<sup>11,15,16</sup> However, Ogata, Sawaki, an Ohno observed that peracid epoxidation of alkynes, which ostensibly proceeds through an oxirene, gave products which were inconsistent with a ketocarbene intermediate.<sup>17</sup> They concluded that oxirenes do not interconvert with ketocarbenes and proposed that ketocarbene-ketocarbene interconversion proceeds through an intramolecular ylide. Lewars' recent example, however, suggests that isomeri-

(1) Hudlicky, T.; Reddy, D. B.; Govindan, S. V.; Kulp, T.; Still, B.; Sheth, J. P. *J. Org. Chem.* **1983**, *48*, 3422–3428. Hudlicky, T.; Kutchan, T. M.; Wilson, S. R.; Mao, D. T. *J. Am. Chem. Soc.* **1980**, *102*, 6351–6353.

(2) March, J. "Advanced Organic Chemistry"; McGraw-Hill: New York, 1977; pp 995–997.

(3) Redmore, D.; Gutsche, C. D. *Adv. Alicyclic Chem.* **1971**, *3*, 125–136. See also Kirmse (ref 5a) p 485.

(4) Steppan, H.; Buhr, G.; Vollmann, H. *Angew. Chem., Int. Ed. Engl.* **1982**, *21*, 455–469. Thompson, L. F.; Willson, C. G.; Bowden, M. J. S. "Introduction to Microlithography: Theory, Materials and Processing"; American Chemical Society: Washington, D.C., 1984. Deforest, W. S. "Photosensitive Materials and Processes"; McGraw-Hill: New York, 1975. Dinaburg, M. S. "Photosensitive Diazo Compounds"; Focal Press: New York, 1964.

(5) For reviews see: (a) Kirmse, W. "Carbene Chemistry", 2nd ed.; Academic Press: New York, 1971; pp 475–493. (b) Moss, R. A.; Jones, M., Eds; "Carbenes"; Wiley: New York, 1973; Vol. I, pp 117–125. (c) Meier, H.; Zeller, K.-P. *Angew. Chem., Int. Ed. Engl.* **1975**, *14*, 32–43. (d) Ando, W. In "The Chemistry of Diazonium and Diazo Groups"; Patai, S., Ed.; Wiley: New York, 1978; Vol. I.

(6) Nakamura, K.; Udagawa, S.; Honda, K. *Chem. Lett.* **1972**, 763–766.

(7) Bolsing, F.; Spanuth, E. *Z. Naturforsch B: Anorg. Chem., Organ. Chem.* **1976**, *31B*, 1391–1396.

(8) Roth, H. D.; Manion, M. L. *J. Am. Chem. Soc.* **1976**, *98*, 3392–3393. Roth, H. D. *Acc. Chem. Res.* **1977**, *10*, 85–91.

(9) Kaplan, F.; Meloy, G. K. *J. Am. Chem. Soc.* **1966**, *88*, 950–956. Kaplan, F.; Mitchell, M. L. *Tetrahedron Lett.* **1979**, 759–762.

(10) Tomioka, H.; Okuno, H.; Izawa, Y. *J. Org. Chem.* **1980**, *45*, 5278–5283. Tomioka, H.; Kondo, M.; Izawa, Y. *J. Org. Chem.* **1981**, *46*, 1090–1094.

(11) The oxirene literature has been comprehensively reviewed recently: Lewars, E. G. *Chem. Rev.* **1983**, *83*, 519–534. Torres, M.; Lown, E. M.; Gunning, H. E.; Strausz, O. P. *Pure Appl. Chem.* **1980**, *52*, 1623–1643.

(12) Tomioka, H.; Okuno, H.; Kondo, S.; Izawa, Y. *J. Am. Chem. Soc.* **1980**, *102*, 7125–7126.

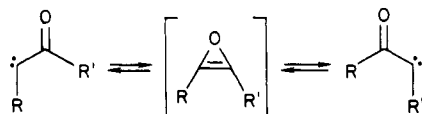
(13) An important control experiment ruled out label scrambling at the diazo ketone stage in azibenzil: Blaustein, M. A.; Berson, J. A. *Tetrahedron Lett.* **1981**, 1081–1084.

(14) Torres, M.; Ribo, J.; Clement, A.; Strausz, O. P. *Can. J. Chem.* **1983**, *61*, 996–998.

(15) Harding, L. B. *J. Am. Chem. Soc.* **1981**, *103*, 7469–7475. See also: Kohler, H. J.; Lischka, H. *J. Am. Chem. Soc.* **1982**, *104*, 5884–5889. Altman, J. A.; Csizmadia, I. G.; Yates, K. *J. Am. Chem. Soc.* **1974**, *96*, 4196–4201.

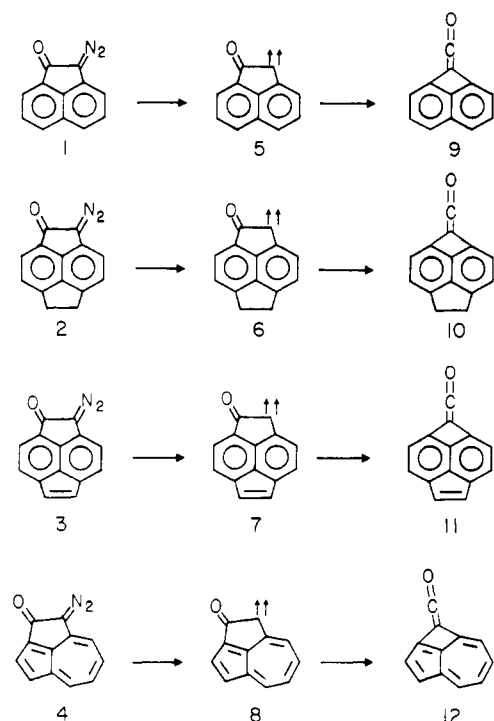
(16) Tanaka, K.; Yoshimine, M. *J. Am. Chem. Soc.* **1980**, *102*, 7655–7662. Bargon, J.; Tanaka, K.; Yoshimine, M. In "Computational Methods in Chemistry"; Bargon, J., Ed.; Plenum: New York, 1980.

(17) Ogata, Y.; Sawaki, Y.; Ohno, T. *J. Am. Chem. Soc.* **1982**, *104*, 216–219.



<sup>†</sup> Dedicated to the memory of Professor Robert V. Stevens.

## Scheme I



zation of an oxirene to a ketocarbene does occur.<sup>18</sup>

Despite intensive efforts, direct experimental evidence for oxirene formation is weak. Meier mentioned isolation of a methanol-trapping product of an oxirene in his review article.<sup>11,19,20</sup> The Strausz group reported the infrared characterization of both bis(trifluoromethyl)oxirene and (trifluoroacetyl)(trifluoromethyl)carbene under matrix-isolation conditions in 1983.<sup>23</sup> However, Lemal and co-workers demonstrated that the species originally assigned as the  $\alpha$ -ketocarbene is actually the  $\alpha$ -keto-diazirine isomer of the  $\alpha$ -diazo ketone starting material.<sup>24</sup> In addition, they failed to generate the oxirene under irradiation conditions, which were similar but not identical with those of Strausz.

We sought a system in which the chemistry and spectroscopy of an  $\alpha$ -ketocarbene could be studied.<sup>25</sup> Shechter<sup>26</sup> and Trost<sup>27</sup> have shown that increasing strain in the transition state for ring contraction will suppress Wolff rearrangement. The absence of Wolff rearrangement chemistry from diazo ketone **1** either thermally or photochemically in solution or thermally in the gas phase<sup>26</sup> suggested that diazo ketone **1** and its analogues **2**, **3**, and **4** should be ideal precursors that impose increasingly severe strain limitations. This turned out to be correct. In this report, we describe the first thorough spectroscopic characterization of  $\alpha$ -ketocarbenes and the first unambiguous examples of nonconcerted Wolff rearrangements which occur upon photolysis of triplet  $\alpha$ -ketocarbenes.

(18) Lewars, E.; Siddiqi, S. *J. Org. Chem.* **1985**, *50*, 135–136.

(19) Meier, H. *IVth IUPAC Symposium on Photochemistry*, 1972, p 163.

(20) For two key experimental studies, which failed to produce oxirene, see ref 21 and 22.

(21) Maier, G.; Reisenauer, H. P.; Sayrac, T. *Chem. Ber.* **1982**, *115*, 2192–2201.

(22) Maier, G.; Sayrac, T.; Reisenauer, H. P. *Chem. Ber.* **1982**, *115*, 2202–2213.

(23) Torres, M.; Bourdelande, J. L.; Clement, A.; Strausz, O. P. *J. Am. Chem. Soc.* **1983**, *105*, 1698–1700.

(24) Laganis, E. D.; Janik, D. S.; Curphey, T. J.; Lemal, D. M. *J. Am. Chem. Soc.* **1983**, *105*, 7457–7459.

(25) For a preliminary report of this work see: Hayes, R. A.; Hess, T. C.; McMahon, R. J.; Chapman, O. L. *J. Am. Chem. Soc.* **1983**, *105*, 7786–7787.

(26) Chang, S.-J.; Ravi Shankar, B. K.; Shechter, H. *J. Org. Chem.* **1982**, *47*, 4226–4234 and references therein.

(27) Trost, B. M.; Kinson, P. L. *Tetrahedron Lett.* **1973**, 2675–2678. Trost, B. M.; Kinson, P. L. *J. Am. Chem. Soc.* **1975**, *97*, 2438–2449.

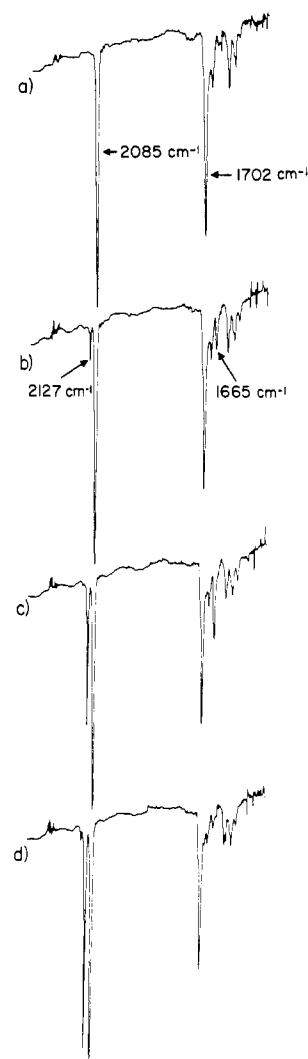


**Figure 1.** Infrared spectra (2500–1500  $\text{cm}^{-1}$ ) obtained upon photolysis of diazo ketone **1** matrix-isolated in argon at 12 K: (a) **1** prior to irradiation; (b) 365  $\pm$  8 nm, 15 min; (c) 365  $\pm$  8 nm, 45 min; (d) 625  $\pm$  8 nm, 182 min. Diazo ketone **1** (2085, 1702  $\text{cm}^{-1}$ ), ketocarbene **5** (1665  $\text{cm}^{-1}$ ), and ketene **9** (2127  $\text{cm}^{-1}$ ) are observed.

## Results

**2-Diazo-1(2H)-acenaphthyleneone (1).** Irradiation (>416 nm, 415 min) of diazo ketone **1** matrix isolated in argon at 15 K gave ketone **9**. Irradiation at shorter wavelengths resulted only in faster conversion of starting material. The structural assignment is based on the intense infrared ketene stretching vibration ( $\nu_{\text{C}=\text{C}=\text{O}}$ ) at 2127  $\text{cm}^{-1}$ . Irradiation (>364 nm, 10 min) of **1** gave a very weak triplet carbene spectrum as observed by ESR spectroscopy. The intensity of the signal did not increase under any irradiation conditions in which cutoff filters were employed (Scheme I). (This occurs when primary photoproducts absorb at longer wavelengths than the starting material.) However, bandpass irradiation (365  $\pm$  8 nm) produced an intense signal due to ketocarbene **5**,  $D/hc = 0.406 \text{ cm}^{-1}$  and  $E/hc = 0.0264 \text{ cm}^{-1}$  ( $Z_1$  990G,  $X_2$  4491G,  $Y_2$  5538G,  $Z_2$  7632G, microwave frequency = 9.255 GHz). After annealing the matrix containing **5** by warming from 15 to 28 K over 12 min, the Curie Law was obeyed upon cooling to 18 K and rewarming to 27 K. Observation of the ESR signal of ketocarbene **5** implies the triplet state is either the ground state or within several cal/mol of the ground state. Irradiation of **5** at long wavelength (625  $\pm$  8 nm) resulted in the irreversible disappearance of the ESR signal. The generation of such an intense ESR spectrum of **5** suggested that **5** should be observable by other methods of spectroscopy as well. Irradiation (365  $\pm$  8 nm, 45 min) of diazo ketone **1** matrix isolated in argon gave the ketocarbene visible absorption spectrum ( $\lambda_{\text{max}}$  621.3, 597.1, 590.3,

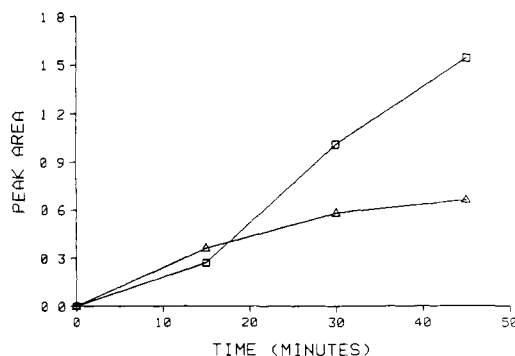


**Figure 2.** Rates of appearance of ketocarbene **5** ( $\Delta$ ) and ketene **9** ( $\square$ ) obtained upon irradiation ( $365 \pm 8$  nm) of diazo ketone **1** matrix isolated in argon at 12 K.

573.4, 563.2 nm). From the position of the (0,0) transition (621.3 nm), we calculate the energy of the  $T_0-T_1$  excitation to be 47 kcal/mol. Subsequent irradiation at long wavelength ( $625 \pm 8$  nm, 62 min) caused a rapid decrease in intensity of the visible absorption spectrum. Irradiation ( $365 \pm 8$  nm) of diazo ketone **1** produced ketene **9** and a species with infrared bands at 1665, 1015, and  $767\text{ cm}^{-1}$ . Monitoring the reaction as a function of irradiation time revealed that the  $1665\text{-cm}^{-1}$  band grew in more rapidly than the ketene band at  $2127\text{ cm}^{-1}$  (Figures 1 and 2). Continued irradiation produced a photostationary concentration of the  $1665\text{-cm}^{-1}$  species. Irradiation at long wavelength ( $625 \pm 8$  nm) resulted in disappearance of the  $1665\text{-}$ ,  $1015\text{-}$ , and  $767\text{-cm}^{-1}$  bands and in growth of the  $2127\text{-cm}^{-1}$  ketene band (Figure 1). Residual diazo ketone **1** was unreactive under these irradiation conditions.

Chemical trapping is often a useful method of confirming structures of intermediates assigned on the basis of spectroscopic data. This can be accomplished under matrix isolation conditions by doping the argon with up to a few percent of a trapping agent. Molecular oxygen as a chemical trap offers the advantage that it does not obscure any region of the infrared spectrum. Irradiation ( $>416$  nm, 400 min) of diazo ketone **1** in an argon/oxygen (80:20) matrix gave 1,8-naphthalic anhydride (**13**) as the primary photoproduct (ca. 5% ketene **9**). The structural assignment of **13** was confirmed by comparison of the infrared spectrum with that of the authentic material (Aldrich) matrix isolated in argon at 15 K (Scheme II). Carbon monoxide is quite useful for trapping carbenes as ketenes, although at high dopant concentrations, the  $\text{C}=\text{O}$  stretch ( $2140\text{ cm}^{-1}$ ) often obscures the ketene stretch ( $\sim 2100\text{ cm}^{-1}$ ) of the trapped product. Irradiation ( $>338$  nm, 200 min) of diazo ketone **1** in an argon/carbon monoxide (99.75:0.25) matrix gave both Wolff rearrangement product (ketene **9**) and trapping product (ketoketene **14**). Again, the Wolff rearrangement could be almost totally suppressed (ca. 5% ketene **9**) by increasing the carbon monoxide concentration to 90:10 (Figure 3). The identity of the ketoketene trapping product **14** was determined by comparison of the infrared spectrum with that of the authentic material prepared independently by Wolff rearrangement of diazo diketone **15** matrix isolated in argon ( $>280$  nm, 60 min) (Figure 3).

**2-Diazo-5,6-Dihydrocyclopent[fg]acenaphthylen-1-one (2).** Irradiation ( $>406$  nm, 500 min) of diazo ketone **2** matrix isolated in argon at 15 K gave Wolff rearrangement, as established by the appearance of the ketene band ( $\nu_{\text{C}=\text{O}}$ ,  $2127\text{ cm}^{-1}$ ) in the infrared spectrum. Band-pass irradiation of **2** ( $390 \pm 8$  nm) produced a mixture of ketocarbene **6** and ketene **10**. Ketocarbene **6** was characterized by its carbonyl stretch ( $1658\text{ cm}^{-1}$ ), its visible absorption spectrum ( $\lambda_{\text{max}}$  643, 639, 626, 619, 617, 611, 600, 594, 588, 583, 580, 574 nm), and its electron spin resonance spectrum ( $D/hc = 0.401\text{ cm}^{-1}$ ,  $E/hc = 0.0253\text{ cm}^{-1}$ ,  $Z_1$  930G,  $X_2$  4506G,  $Y_2$  5506G,  $Z_2$  7581G, microwave frequency = 9.259 GHz). The Curie law was obeyed in the temperature range 16–26 K. Observation of the ESR signal of ketocarbene **6** implies the triplet state is either the ground state or within several cal/mol of the ground state. Initially, the  $1658\text{-cm}^{-1}$  infrared band of **6** grew

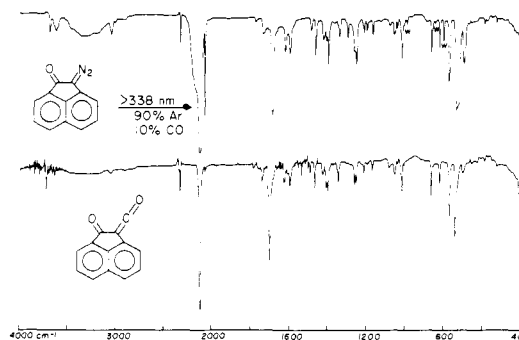
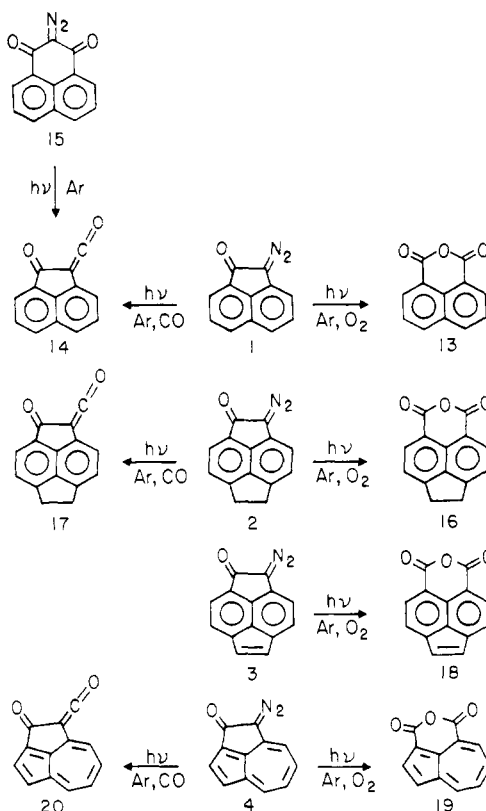


**Figure 3.** Top: infrared spectrum of ketoketene **14** obtained upon irradiation of diazo ketone **1** in a 10% CO-doped argon matrix at 12 K. Bands marked **w** are due to Wolff rearrangement product (ketene **9**). Bottom: infrared spectrum of ketoketene **14** obtained upon irradiation of diazo diketone **15** matrix-isolated in argon at 12 K.

#### Scheme II



in more rapidly than the  $2127\text{-cm}^{-1}$  band of ketene **10** before leveling off at a photostationary concentration. From the position of the (0,0) transition (643 nm), we calculate the energy of the  $T_0-T_1$  excitation to be 44 kcal/mol.

Long-wavelength irradiation of  $\alpha$ -ketocarbene **6** ( $640 \pm 8$  nm) produced (1) a slow decrease in the ESR signal, the visible spectrum, and the  $1658\text{-cm}^{-1}$  infrared band of **6**, (2) a slow increase in intensity of the  $2127\text{-cm}^{-1}$  infrared band of ketene **10**, and (3) a slow increase in the  $2088\text{-cm}^{-1}$  infrared band and 393-nm visible absorption of diazo ketone **2**. Shorter wavelength irradiation of **6** ( $>574$  nm) resulted in a much more rapid decrease in the ESR, UV, and IR signals of **6** and in exclusive formation of ketene **10**. Diazo ketone **2** is unreactive under these irradiation conditions.

Anhydride **16** formation occurred upon irradiation ( $>416$  nm, 1100 min) of **2** in an argon/oxygen matrix (80:20). The identity of **16** was confirmed by comparison with the infrared spectrum of the independently prepared material (KBr pellet).<sup>28</sup> Similarly, irradiation ( $>416$  nm, 1000 min) of **2** in an argon/carbon mon-

(28) Synthesized by the method of Carpino and Gowecke<sup>29</sup> as modified by Trost.<sup>30</sup>

**Table I.** Carbonyl Absorptions of Acenaphthene and Cyclopent[*cd*]azulene Derivatives<sup>a</sup>

	1710 cm <sup>-1</sup>		1665 cm <sup>-1</sup>
	1720 cm <sup>-1</sup>		1733 cm <sup>-1</sup> 1685 cm <sup>-1</sup>
	1705 cm <sup>-1</sup> <sup>b</sup>		1680 cm <sup>-1</sup>

<sup>a</sup>All spectra obtained as KBr pellets, unless otherwise noted.<sup>b</sup>Argon matrix isolated at 12 K.

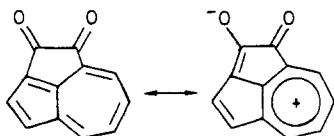
oxide matrix (99.75:0.25) did not give ketene **10**. The assignment of the trapping product as ketotene **17** must remain tentative, as no independent synthesis of **17** is available.

**2-Diazocyclopent[*fg*]acenaphthylene-1-one (3).** Experimental complications precluded a thorough investigation of the photochemistry of diazo ketone **3**. The strong UV absorption of ketene **11** forced the use of tedious layering experiments (see Experimental Section) to circumvent the problem of internal filtering. Irradiation (>220 nm) of diazo ketone **3** matrix isolated in argon at 15 K gave rise to Wolff rearrangement, as established by the appearance of the ketene band ( $\nu_{\text{C}=\text{O}}$ , 2128 cm<sup>-1</sup>) in the infrared spectrum.

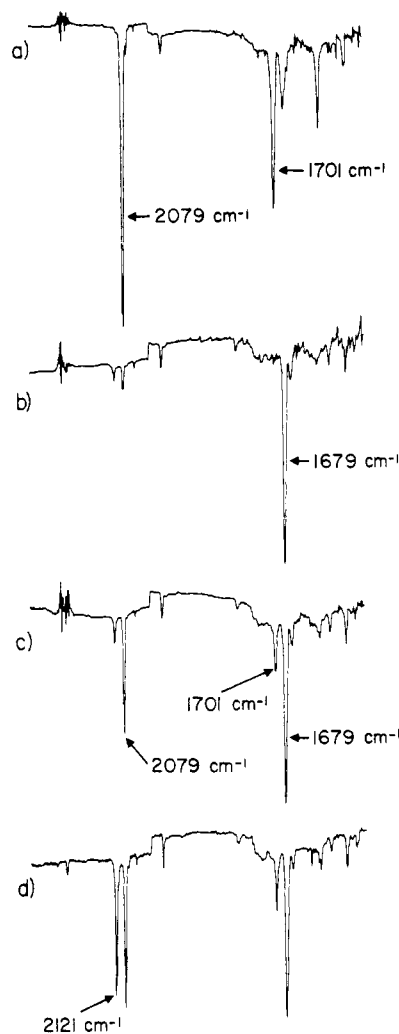
The ketocarbene intermediate (**7**) was not characterized spectroscopically. However, a second product (ca. 25%) observed in the infrared spectrum of the photolysis mixture was assigned to anhydride **18** by comparison with the infrared spectrum of the independently prepared material (KBr pellet).<sup>29</sup> Anhydride **8** formation is presumably due to reaction of ketocarbene **7** with molecular oxygen impurity in the argon matrix. (Traces of anhydride were also observed with diazo ketones **1** and **2**, but much more anhydride is observed in this case due to the nature of the layering experiment.)

**1-Diazocyclopent[*cd*]azulene-2-one (4).** Before discussing the chemistry of diazo ketone **4**, the question of regiochemistry in the addition of tosylhydrazide to the azulene quinone must be addressed. Infrared spectroscopy provides the answer (Table I). The acenaphthene derivatives clearly demonstrate that the nature of the substituent  $\alpha$  to the carbonyl group does not have much effect on the position of the carbonyl infrared absorption. In the azulene series, the carbonyl groups of the quinone are no longer identical by symmetry, and two carbonyl absorptions are observed (1733, 1685 cm<sup>-1</sup>, Table I). The infrared spectrum of the monoketone **21** (1655 cm<sup>-1</sup>) established that the lower frequency carbonyl band is due to the ketone at the 2-position. Diazo ketone **4** exhibits a carbonyl absorption at a similar frequency (1680 cm<sup>-1</sup>). Therefore, the ketone must also be at the 2-position.

The infrared data also offer insight into the reason behind the observed regioselectivity. The ketone at the 2-position of the quinone is highly conjugated, due to the contribution of the



resonance structure, which contains a tropylium cation. This

(29) Carpino, L. A.; Gowecke, S. *J. Org. Chem.* **1964**, *29*, 2824–2830.(30) Trost, B. M.; Bright, G. M.; Frihart, C.; Brittell, D. *J. Am. Chem. Soc.* **1971**, *93*, 737–745.

**Figure 4.** Infrared spectra (2500–1500 cm<sup>-1</sup>) obtained upon photolysis of diazo ketone **4** matrix isolated in argon at 12 K: (a) **4** prior to irradiation; (b) >415 nm, 30 min; (c) >554 nm, 330 min; (d) >554 nm, 64 h. Diazo ketone **4** (2079, 1701 cm<sup>-1</sup>), ketocarbene **8** (1679 cm<sup>-1</sup>), and ketene **12** (2121 cm<sup>-1</sup>) are observed.

explains why the carbonyl at the 2-position is at lower frequency than the carbonyl at the 1-position. It also explains why reaction occurs at the less conjugated, more reactive ketone at the 1-position.

Irradiation (>416 nm, 60 min) of diazo ketone **4** matrix isolated in argon at 12 K produced ketocarbene **8** cleanly. No ketene **12** was observed under these conditions. This is in contrast to diazo ketones **1** and **2**, which each required band-pass irradiation to produce detectable quantities of ketocarbenes **5** and **6**. Even then, the ketocarbenes were produced only as mixtures with the ketenes **9** and **10**. Ketocarbene **8** was characterized by its infrared spectrum (1679 s, 1664 w, 1620 w, 1579 m, 1542 m, 1520 m, 1451 w, 1438 w, 1424 w, 1412 w, 1391 m, 1349 w, 1320 m, 1286 w, 1242 w, 1193 m, 1148 m, 1060 w, 991 m, 795 m, 741 w, 736 w, 637 w, 632 w, 602 w, 558 w, 575 w cm<sup>-1</sup>; Figure 4), its visible absorption spectrum ( $\lambda_{\text{max}}$  663, 644, 635, 620, 609, 602, 579, 551, 527, 474 nm; Figure 5), and its electron spin resonance spectrum ( $D/hc = 0.427$  cm<sup>-1</sup>,  $E/hc = 0.0179$  cm<sup>-1</sup>,  $Z_1$  1239G,  $X_2$  4733G,  $Y_2$  5443G,  $Z_2$  7871G, microwave frequency = 9.234 GHz, Figure 6). Observation of the ESR signal of ketocarbene **8** implies the triplet state is either the ground state or within several cal/mol of the ground state. From the position of the (0,0) transition (663 nm), we calculate the energy of the T<sub>0</sub>-T<sub>1</sub> excitation to be 43 kcal/mol.

Long-wavelength irradiation of **8** (>554 nm, 64 h) produced a slow decrease in intensity of the IR and visible spectrum of **8**, a slow increase in intensity of the IR and visible spectra of diazo ketone **4**, and an extremely slow increase in intensity of the IR

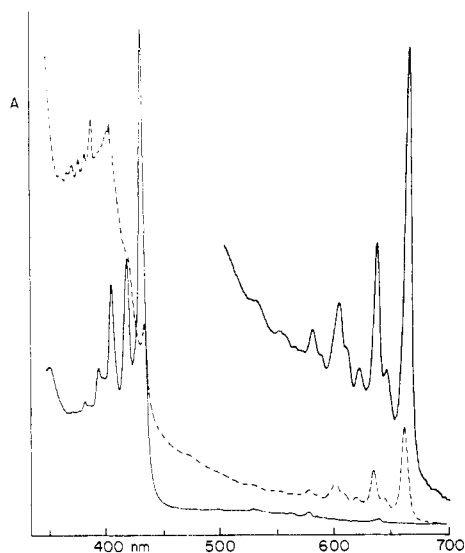


**Figure 5.** Solid line: UV-vis spectrum of diazo ketone **4** matrix isolated in argon at 12 K. Broken line: UV-vis spectrum of ketocarbene **8** obtained upon irradiation (>416 nm, 60 min) of **4**. Inset: expansion of the  $\pi, \pi^*$  transition of ketocarbene **8**.

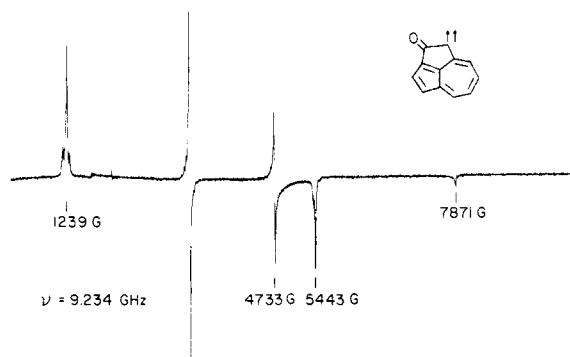
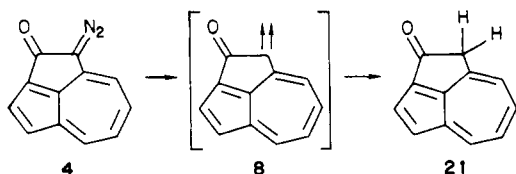


**Figure 6.** Electron spin resonance spectrum of ketocarbene **8** obtained upon irradiation (>406 nm, 1306 min) of argon matrix-isolated **4**. The matrix has been annealed by warming to 38 K and recooled to 21 K.

spectrum of ketene **12** (Figure 4). In contrast, short-wavelength irradiation of **8** (>300 nm, 120 min) resulted in the disappearance of the IR, visible, and ESR spectra of **8** and in the appearance of the infrared and visible spectra of ketene **12**.

Irradiation of diazo ketone **4** (>416 nm, 70 min) in an argon/oxygen (90:10) matrix gave rise to 1,8-azulene dicarboxylic acid anhydride (**19**), presumably via oxygen trapping of ketocarbene **8** followed by rearrangement. The identity of **19** was verified by comparison of the infrared spectrum with that of an authentic sample of **19**<sup>31</sup> matrix isolated in argon. Irradiation (>406 nm, 57 h) of **4** in an argon/carbon monoxide (99.75:0.25) matrix generated ketoketene **20** (2135  $\text{cm}^{-1}$ , 1675  $\text{cm}^{-1}$ ). No independent synthesis of **20** is available to confirm the structural assignment.

Flash vacuum thermolysis (400 °C) of **4** followed by matrix isolation of the pyrolysate in argon at 15 K did not produce ketene **12**. Rather it produced ketone **21**, a product of double hydrogen atom abstraction by ketocarbene **8**. The identity of **21** was established by comparison of its infrared spectrum with that of the authentic material<sup>32</sup> matrix isolated in argon.



(31) Hafner, K.; Dieter, R.; Krimmer, H.-P., unpublished results.

**Table II.**  $D$  Values of Selected Carbenes<sup>a</sup>

Carbene	$D/hc$ ( $\text{cm}^{-1}$ )	Carbene	$D/hc$ ( $\text{cm}^{-1}$ )
$\text{CF}_3\dot{\text{C}}\text{H}$	0.712	$\text{Ph}\dot{\text{C}}\text{H}$	0.515
$\text{CF}_3\dot{\text{C}}\text{CF}_3$	0.744	$\text{Ph}\dot{\text{C}}\text{CH}_2\text{Ph}$	0.493
$\text{CF}_3\dot{\text{C}}(\text{O})\text{CF}_3$	0.572 <sup>b,c</sup>	$\text{Ph}\dot{\text{C}}\text{Ph}$	0.405
		$\text{Ph}\dot{\text{C}}(\text{O})\text{Ph}$	0.312 <sup>b,c</sup>

<sup>a</sup> Values taken from Kirmse (ref 5a, p 201), unless otherwise noted.

<sup>b</sup>  $D$  value is for rotomer **22**. <sup>c</sup> Murai et al. (ref 35).

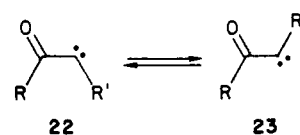
**Table III.** Zero-Field Splitting Parameters of Cyclic Carbenes

Carbene	$D/hc$ ( $\text{cm}^{-1}$ )	$E/hc$ ( $\text{cm}^{-1}$ )	Ref.
	0.409	0.0120	a
	0.378	0.0160	a
	0.408	0.0283	a
	0.405	0.0194	a
	0.38		36
	0.384	0.0247	42
	0.387	0.0158	42

<sup>a</sup> Kirmse (ref 5a), p 201.

## Discussion

Few ESR spectra of  $\alpha$ -carbonylcarbenes have been obtained.<sup>33-38</sup> Most  $\alpha$ -carbonylcarbenes reported in the literature exist as pairs of rotational isomers (**22** and **23**).<sup>39</sup> Because the carbenes studied in this work are cyclic, only rotomer **22** is relevant to this discussion. The carbonyl group delocalizes some of the  $\pi$ -electron



spin density for the carbene center, as shown by the smaller  $D$  values relative to the model compounds without carbonyl groups (Table II). However, the nature of the substituents is clearly the predominant factor affecting the  $D$  values. This suggests that 1-naphthylcarbene might be a good model for our systems.

Table III contains the only 5-membered-ring carbenes studied by ESR spectroscopy. Placing the carbene in a 5-membered ring

(32) Hafner, K.; Meinhardt, K.-P.; Richarz, W. *Angew. Chem., Int. Ed. Engl.* **1974**, *13*, 204-205.

(33) Trozzolo, A. M.; Fahrenholtz, S. R. *Abstr. Pap. Am. Chem. Soc. 151st* **1966**, K23. Trozzolo, A. M. *Acc. Chem. Res.* **1968**, *1*, 329-335.

(34) Hutton, R. S.; Roth, H. D. *J. Am. Chem. Soc.* **1978**, *100*, 4324-4325.

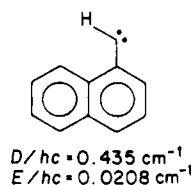
(35) Murai, H.; Ribo, J.; Torres, M.; Strausz, O. P. *J. Am. Chem. Soc.* **1981**, *103*, 6422-6426.

(36) Moriconi, E. J.; Murray, J. J. *J. Org. Chem.* **1964**, *29*, 3577-3584.

(37) Wasserman and Murray studied derivatives of cyclohexa-2,5-dien-1-on-4-ylidene. Wasserman, E.; Murray, R. W. *J. Am. Chem. Soc.* **1964**, *86*, 4203-4204.

(38) The  $D$  value reported for dibenzoylmethylene (Murai, H.; Torres, M.; Strausz, O. P. *Chem. Phys. Lett.* **1980**, *70*, 358-360) is anomalously small compared with other  $\alpha$ -carbonylcarbenes.<sup>33-37</sup>

(39) It is confusing that Roth<sup>34</sup> and Strausz<sup>35</sup> use opposite conventions in assigning cis and trans nomenclature to the rotameric structures.



decreases the bond angle from the value normally found in unconstrained triplet carbenes. However, this appears to have little effect on the  $D$  value, as shown by the similar  $D$  values of diphenylcarbene ( $0.405 \text{ cm}^{-1}$ ) and fluorenylidene ( $0.408 \text{ cm}^{-1}$ ). Again, this indicates that 1-naphthylcarbene is a good model.

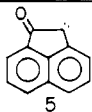
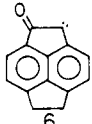
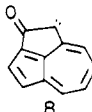
The zero-field splitting parameters<sup>40</sup> assigned to  $\alpha$ -ketocarbenes **5** and **6** (Table IV) are reasonable on the basis of the model of 1-naphthylcarbene with a smaller  $D$  value caused by the presence of an  $\alpha$ -carbonyl group. It is also reasonable that the  $D$  values of **5** and **6** are larger than the  $\alpha,\beta$ -unsaturated- $\gamma$ -ketocarbenes of Chapman and Abelt.<sup>42</sup> Delocalization of spin density to oxygen in these systems represents a large separation of the electrons in space and results in rather small  $D$  values. No good model systems exist for comparison with the zero-field splitting parameters of **8** (Table IV).

The observation of triplet  $\alpha$ -ketocarbenes **5**, **6**, and **8** by ESR spectroscopy is of significance. Schuster and co-workers attributed the small  $T_0$ - $S_1$  gap of 1.1 kcal/mol in fluorenylidene to angle bending in the 5-membered ring.<sup>43</sup> (Typical singlet-triplet splittings in acyclic arylcarbenes are of the order of 4–6 kcal/mol.)<sup>44</sup> While our data do not bear directly on the magnitude of the  $T_0$ - $S_1$  splitting, they do suggest that the angle strain in **5**, **6**, and **8** has not caused the triplet state to rise above the singlet state in energy.

The UV-vis spectra obtained upon irradiation of diazo ketones **1**, **2**, and **4** provide strong confirmation of the ketocarbene structural assignment. Although these are the first UV-vis spectra reported for triplet  $\alpha$ -ketocarbenes, they contain the weak  $\pi,\pi^*$  transitions with extensive vibronic coupling that are characteristic of triplet arylcarbenes<sup>33,45</sup> (and the benzyl radical).<sup>46</sup> Our experimental technique does not permit evaluation of extinction coefficients; however, the amount of sample required to obtain a good visible spectrum is roughly the same as that required to obtain an infrared spectrum. The extinction coefficients for the  $\pi,\pi^*$  transition are thus of the order of 10–100. Ultraviolet spectra in the region of the aromatic absorptions (200–350 nm) were not obtained.

The infrared spectra of **5**, **6**, and **8** are also consistent with the ketocarbene structural assignment. These are the first reported observations of an  $\alpha$ -ketocarbene by infrared spectra. The electron-deficient, divalent carbon center weakens the adjacent carbon-oxygen double bond. Therefore, the carbonyl absorptions of the ketocarbenes (**5**,  $1665 \text{ cm}^{-1}$ , **6**,  $1658 \text{ cm}^{-1}$ , **8**  $1679 \text{ cm}^{-1}$ ) shift to lower frequencies than the carbonyl absorptions of the starting diazo ketones (**1**,  $1702 \text{ cm}^{-1}$ ; **2**,  $1704 \text{ cm}^{-1}$ , **4**,  $1702 \text{ cm}^{-1}$ ). We specifically rule out a ketodiazirine structure, as the carbonyl bands of  $\alpha$ -ketodiazirines and  $\alpha$ -amidodiazirines shift to higher frequencies than their corresponding  $\alpha$ -diazo ketone and  $\alpha$ -diazo

Table IV. Zero-Field Splitting Parameters of  $\alpha$ -Ketocarbenes

Carbene	$D/hc$ ( $\text{cm}^{-1}$ )	$E/hc$ ( $\text{cm}^{-1}$ )
 5	0.406	0.0264
 6	0.401	0.0253
 8	0.427	0.0178

amide isomers.<sup>47,48</sup> The ca.  $1670\text{-cm}^{-1}$  bands could be due to the weak  $\text{N}=\text{N}$  stretch of an  $\alpha$ -ketodiazirine. We reject this possibility because we did not observe an intense carbonyl band above  $1700 \text{ cm}^{-1}$ .

Infrared spectroscopy clearly establishes that  $\alpha$ -ketocarbene **8** is the primary photoproduct obtained upon irradiation of diazo ketone **4**, as no ketene **12** is formed under these conditions (Figure 4). Two lines of argument lead to the conclusion that the  $\alpha$ -ketocarbenes **5–7** are also the primary photoproducts obtained upon irradiation of diazo ketones **1–3**. First, infrared monitoring of ketocarbene and ketene appearance as a function of irradiation time shows that ketocarbenes **5** and **6** form faster than ketenes **9** and **10** (Figures 1 and 2). Second, irradiation of diazo ketones **1–3** in argon matrices doped with carbon monoxide or oxygen results in suppression of Wolff rearrangement product (Figure 3). At low dopant concentration, the ketocarbenes partition between reaction with dopant or ring contraction; at high dopant concentrations, ring contraction is virtually eliminated.<sup>50</sup> This also enables us to rule out a situation in which diazo ketone partitions between concerted ring contraction (to give ketene) and simple nitrogen loss (to give ketocarbene).

To summarize the experimental facts, ketocarbenes **5–8** are the primary photoproducts of diazo ketones **1–4**, and ketocarbenes **5–8** photochemically produce ketenes **9–12**. This is the first direct observation of nonconcerted Wolff rearrangements which proceed through  $\alpha$ -ketocarbene intermediates.

Our results contain mechanistic implications for the detailed photophysics of the Wolff rearrangement. We have shown that triplet ground-state ( $T_0$ ) ketocarbene is the primary photoproduct of the diazo ketone precursor in each of the four cases studied. Therefore, either  $S'$  ketocarbene<sup>55</sup> is not involved in going from

(47) Miyashi, T.; Nakajo, T.; Mukai, T. *J. Chem. Soc., Chem. Commun.* **1978**, 442–443. Franich, R. A.; Lowe, G.; Parker, J. *J. Chem. Soc., Perkin Trans 1*, **1972**, 2034–2041. Lowe, G.; Parker, J. *J. Chem. Soc. D*, **1971**, 1135–1136. Voigt, E.; Meier, H. *Angew. Chem., Int. Ed. Engl.* **1975**, *14*, 103–104. Voigt, E.; Meier, H. *Chem. Ber* **1975**, *108*, 3326–3335. Livinghouse, T.; Stevens, R. V. *J. Am. Chem. Soc.* **1978**, *100*, 6479–6482.

(48) As a case in point, 3-diazohexafluoro-2-butanone exhibits a carbonyl band at  $1700\text{--}1720 \text{ cm}^{-1}$ .<sup>49</sup> Irradiation in an argon matrix gives a  $1761 \text{ cm}^{-1}$  carbonyl band of the corresponding  $\alpha$ -ketodiazirine,<sup>24</sup> which had been erroneously attributed to the  $\alpha$ -ketocarbene earlier.<sup>23</sup>

(49) Dyatkin, B. L.; Mochalina, E. P. *Izv. Akad. Nauk. Arm. SSR, Khim. Nauki* **1965**, 1035–1039.

(50) It has been reported that singlet oxygen reacts with diazo ketone **1** in solution to give either anhydride **13** or the diketone plus  $\text{N}_2\text{O}$ .<sup>51</sup> It has also been observed that irradiation ( $>514 \text{ nm}$ ) of diphenyldiazomethane matrix isolated in argon/oxygen (80:20) gives only benzophenone and  $\text{N}_2\text{O}$ .<sup>52</sup> In the present oxygen trapping experiments, neither diketone nor  $\text{N}_2\text{O}$  were observed. We therefore conclude that oxygen reacts with the ketocarbenes **5–8** and not directly with the diazo ketones **1–4**. The mechanism of the oxygen trapping is considered elsewhere.<sup>33,54</sup>

(51) Okada, K.; Mukai, T. *Tetrahedron Lett.* **1980**, 359–360.

(52) Chapman, O. L.; Hess, T. C. *J. Am. Chem. Soc.* **1984**, *106*, 1842–1843.

(53) Chapman, O. L. *Pure Appl. Chem.* **1979**, *51*, 331–339.

(54) Hess, T. C. Ph.D. Dissertation, University of California, Los Angeles, CA, 1978.

(40) The best fit of the observed ESR spectra with the spin Hamiltonian<sup>41</sup> (assuming  $g_x = g_y = g_z = g_e$ ) provided the zero-field splitting parameters.

(41) Wasserman, E.; Snyder, L. C.; Yager, W. A. *J. Chem. Phys.* **1964**, *41*, 1763–1772.

(42) Chapman, O. L.; Abelt, C. J., manuscript in preparation.

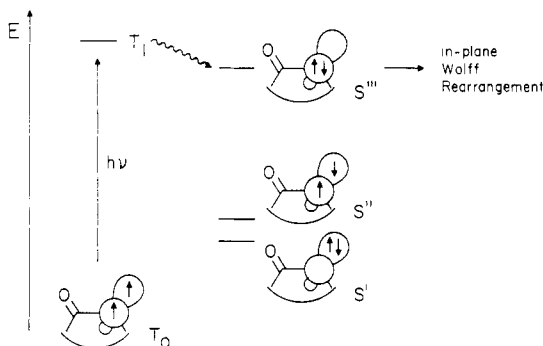
(43) Grasse, P. B.; Brauer, B.-E.; Zupancic, J. J.; Kaufman, K. J.; Schuster, G. B. *J. Am. Chem. Soc.* **1983**, *105*, 6833–6845. Lapin, S. C.; Brauer, B.-E.; Schuster, G. B. *J. Am. Chem. Soc.* **1984**, *106*, 2092–2100.

(44) Closs, G. L.; Rabinow, B. E. *J. Am. Chem. Soc.* **1976**, *98*, 8190–8198. Eisenthal, K. B.; Turro, N. J.; Aikawa, M.; Butcher, J. A.; DuPuy, C.; Hefferon, G.; Heatherington, W.; Korenowski, G. M.; McAuliffe, M. J. *J. Am. Chem. Soc.* **1980**, *102*, 6563–6565. DuPuy, C.; Korenowski, G. M.; McAuliffe, M.; Heatherington, W. M.; Eisenthal, K. B. *Chem. Phys. Lett.* **1981**, *77*, 272–274.

(45) West, P. R.; Chapman, O. L.; LeRoux, J.-P. *J. Am. Chem. Soc.* **1982**, *104*, 1779–1782.

(46) Porter, G.; Strachan, E. *Spectrochim. Acta* **1958**, *12*, 299–304. Andrews, L.; Miller, J. H.; Keelan, B. W. *Chem. Phys. Lett.* **1980**, *71*, 207–210.

$S_1(n, \pi^*)$  or  $S_2(\pi, \pi^*)$  diazo ketone to  $T_0$  ketocarbene (which is contrary to the "conventional wisdom" for such processes<sup>55</sup>) or intersystem crossing of  $S'$  to  $T_0$  is fast compared to Wolff rearrangement (which implies that  $S'$  is unreactive with respect to Wolff rearrangement). Considerable evidence suggests that Wolff rearrangement occurs in a singlet state.<sup>5,56</sup> This argues against Wolff rearrangement proceeding through  $T_0$  and  $T_1$  in our systems. Furthermore, calculations predict high barriers for 1,2-shifts in  $T_0$  methylcarbene.<sup>15</sup> Calculations by Tanaka and Yoshimine<sup>16</sup> and by Radom and co-workers<sup>57</sup> predict no barrier for Wolff



rearrangement in  $S_1$  formylcarbene (which corresponds to the  $S'$  state of our systems<sup>55</sup>). In formylcarbene, simple rotation about the C-C bond can align the vacant p-orbital and the C-H bond in the syn-periplanar conformation required for the 1,2-shift to occur. However, the  $S'$  state of the conformationally rigid ketocarbenes **5-8** cannot achieve such an orientation. Hence,  $S'$  is not the appropriate state for ring contraction.<sup>58</sup> The singlet biradical state,  $S''$ , is inappropriate because it does not possess a vacant orbital. Internal conversion of  $T_1$  to  $S'''$  should be much more efficient than to  $S'$  or  $S''$ , as  $S'$  and  $S''$  lie 30-40 kcal/mol below  $T_1$  in energy. In fact,  $S'''$  is the ideal configuration for in-plane Wolff rearrangement. Bond migration can occur in the plane of the molecule to the back lobe of the vacant  $sp^2$  hybrid orbital. We suggest that  $S'''$  is the reactive state for ketocarbenes **5, 6, 7, and 8**.

Ketocarbene **5** rearranges rapidly via  $S'''$ . Two factors change this for **6** and **8** (presumably **7**, also). First, the absorption maxima of **6** and **8** shift to a longer wavelength than that of **5**. Second, strain in the transition state for ring contraction increases in the series from **5** to **8**. Thus, ketocarbenes **6** and **8** absorb lower energy photons when more energy is required to overcome the strain introduced in the rearrangement. As Wolff rearrangement becomes less and less efficient, readdition of dinitrogen to  $S'''$  ketocarbene can compete with ring contraction. This interpretation requires an additional, upper-excited state to be responsible for the rapid Wolff rearrangement upon short-wavelength irradiation of the ketocarbenes.

Our results indicate that the previously reported failures<sup>26</sup> of diazo ketone **1** to undergo the Wolff rearrangement are not due to ring strain in ketene **9**. Rather, stereoelectronic factors in ketocarbene **5** preclude ring contraction in the  $S'$  state, thereby leading to trapping of the highly-reactive, first-formed ketocarbene **5**. It is quite remarkable that each of the diazo ketones **1-4** does undergo the Wolff rearrangement to give the strained ketenes

(55) The carbene singlet states are designated  $S'$ ,  $S''$ , and  $S'''$  because their position in the singlet manifold relative to singlet states of the aromatic chromophore is not known. The energies increase in the order  $S' < S'' < S'''$ .

(56) Evidence has been presented to indicate that concerted Wolff rearrangement in conformationally mobile systems proceeds via the lowest vibrational state of  $S_1$  diazoketone. Marfisi, C.; Verlaque, P.; Davidovics, G.; Pourcin, J.; Pizzala, L.; Aycard, J.-P.; Bodot, H. *J. Org. Chem.* **1983**, *48*, 533-537.

(57) Bouma, W. J.; Nobes, R. H.; Radom, L.; Woodward, C. E. *J. Org. Chem.* **1982**, *47*, 1869-1875.

(58) A referee suggested that our data can be explained by inefficient ring contraction in the  $S'$  state. However, this postulate disregards stereoelectronic effects and fails to explain the known thermal chemistry of diazoketone **1**. Flash vacuum thermolysis of **1** is expected to produce an equilibrium mixture of singlet ( $S'$ ) and triplet ( $T_0$ ) **5**. Even inefficient ring contraction in  $S'$  should give rise to some ketene **9** under these conditions.<sup>26</sup>

**9-12**. To the best of our knowledge, ketenes **10, 11, and 12** represent the first examples of each type of fused-ring system.

Finally, we obtained no evidence for oxirene participation. Photolysis of the diazo ketones **1-4** produced no infrared bands which could be assigned to an oxirene intermediate. An extensive matrix-isolation study of diazo ketones (including **1**) by Maier and co-workers also failed to produce any evidence of oxirene formation.<sup>20</sup> Furthermore, our ESR studies indicate that irradiation of the unsymmetrical  $\alpha$ -ketocarbene **8** does not result in equilibration with an isomeric  $\alpha$ -ketocarbene. The failure to observe equilibration argues against involvement of an oxirene intermediate or an oxirene-like transition state in these systems.

## Summary

The primary photoproducts obtained upon irradiation of  $\alpha$ -diazo ketones **1-4** are the corresponding  $\alpha$ -ketocarbenes **5-8**. These are the first  $\alpha$ -ketocarbenes to be characterized by infrared and UV-vis spectroscopy. Their ESR spectra have also been obtained. Subsequent irradiation of the  $\alpha$ -ketocarbenes **5-8** results in ring contraction to the strained ketenes **9-12**. The overall conversions of  $\alpha$ -diazo ketone to  $\alpha$ -ketocarbene to ketene provide the first clear-cut examples of nonconcerted Wolff rearrangements. Ring contraction occurs upon photolysis of the ground state triplet ketocarbenes. The rigid geometry of these systems should make the  $S'$  state unreactive with respect to ring contraction. We suggest the  $S'''$  state as the reactive state because bond migration can occur in the plane of the molecule to the back lobe of the vacant  $sp^2$  hybrid orbital. Ketenes **10, 11, and 12** represent the first examples of these fused-ring systems.

## Experimental Section

<sup>1</sup>H NMR spectra were recorded on Varian T-60 or Bruker WP-200 instruments. Chemical shifts ( $\delta$ ) are reported as ppm downfield from internal SiMe<sub>4</sub>. Melting points were determined on a Thomas Hoover Unimelt apparatus in open capillaries and are uncorrected. Elemental analyses were performed by Spang Microanalytical Laboratory (Eagle Harbor, MI). Mass spectra were obtained on AEI MS-9 or MS-902 spectrometers.

Infrared spectroscopy was performed with a Beckman 4250 or a Perkin-Elmer 580B with Model 3600 data station. UV-vis spectroscopy was performed with a Beckman Acta CV or a Perkin-Elmer 330 with Model 3600 data station. ESR spectra were obtained with an X-band spectrometer constructed from a variety of commercial components. The magnetic field was calibrated with an NMR gaussmeter, and the microwave frequency was determined by the use of a DPPH reference.

**Matrix-Isolation Spectroscopy.** The apparatus and experimental technique used in our group for the study of matrix-isolated reactive species have been described in careful detail by Hess<sup>54</sup> and Kreil.<sup>59</sup> The apparatus consists of three components: a refrigeration unit, a vacuum system, and a gas-handling system, all mounted on a moveable cart. An Air Products Model 202 "Displex" cryogenic refrigeration system, equipped with standard instrumentation skirt and optical spectroscopy shroud (Model DMX-1A), provides cooling (Figure 7).

A 25-mm diameter  $\times$  0.5-mm thick spectroscopic window in a chrome-plated, high-conductivity copper holder is attached to the bottom of the second stage of the expander. Indium gaskets provide thermal contact between the window and the holder and the holder and the expander. The window material must be transparent to spectroscopic irradiation, pliable to prevent cracking during heating and cooling cycles, and thermally conducting at cryogenic temperatures. Cesium iodide (or cesium bromide) is the material of choice for infrared experiments, sapphire for UV-vis.

A chrome-plated, high-conductivity copper radiation shield surrounds the second stage of the expander and the window holder. The shield is connected to the first stage of the expander and is cooled to 40 K. The shield traps most of the impurities due to small vacuum leaks and also prevents radiative warming of the matrix.

The window temperature is measured by a 0.07% iron-doped gold vs. chromel thermocouple or a hydrogen vapor bulb. Temperature regulation of the window is achieved by a small resistive heater surrounding the cold tip. The heater is connected to an Air Products, Inc. Model APD-B temperature controller. The controller monitors the temperature via the thermocouple and supplies current to the heater to maintain a preset temperature.

The vacuum system is required to maintain thermal insulation of the cold head. The system consists of a conventional air-cooled, oil-diffusion pump (Edwards Vacuum Components Limited Model E02) backed by

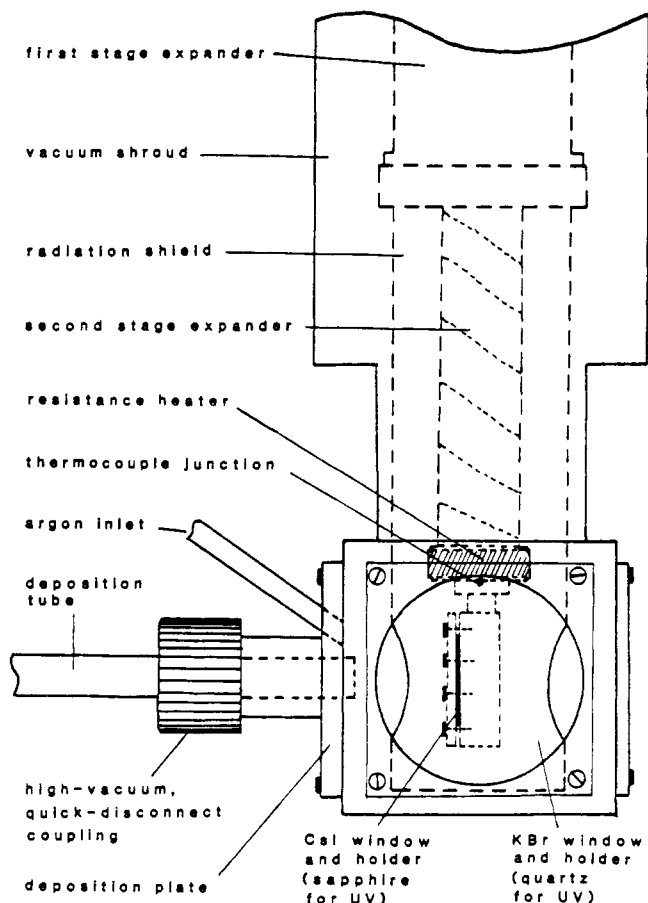


Figure 7. Apparatus for infrared and UV-vis matrix-isolation spectroscopy.

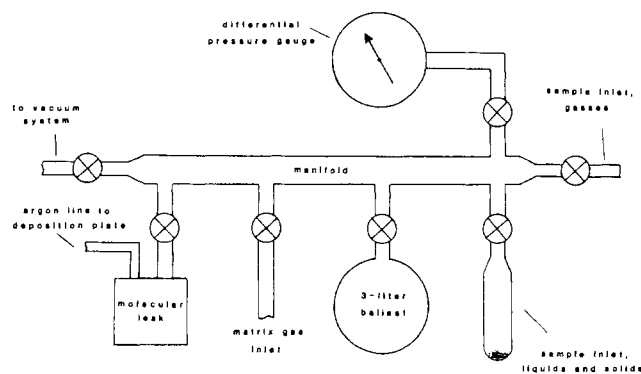


Figure 8. Gas-handling system.

a mechanical forepump (Welch Duo-Seal Model 1402). Soft-soldered copper pipe, brass bellows valves (Veeco Instruments, Inc.), and flexible 321 stainless-steel tubing (Cajon) connect the diffusion pump to the cold head. Pressure is measured by a cold cathode gauge tube (H. S. Martin and Son, Inc.). Pressures less than  $10^{-6}$  torr can be achieved.

A vacuum shroud surrounds the cold head to prevent condensation of the atmosphere onto the cryogenic surfaces. The stainless-steel shroud has four right-angle ports in the window region of the cold tip. Two opposing ports are fitted with windows for spectroscopic viewing (potassium bromide for infrared, quartz for UV-vis). The remaining ports are fitted with a quartz plate for very short wavelength irradiation and a deposition plate for admitting the sample and matrix gas. The windows are tightly clamped to the shroud with aluminum holders. The entire shroud is connected to the cold head by a double O-ring seal. This seal allows shroud rotation through  $90^\circ$  to enable deposition, then spectroscopic observation, and irradiation of the matrix.

The gas handling system (Figure 8) consists of a manifold, a matrix gas inlet, a sample inlet, a 3-L ballast, a differential pressure gauge (Pennwalt Company, Wallace and Tiernan Division, Model 62A-4D-0800), and an outlet to a precision, variable leak (Granville-Phillips; Series 203). The leak is connected to the deposition plate on the vacuum

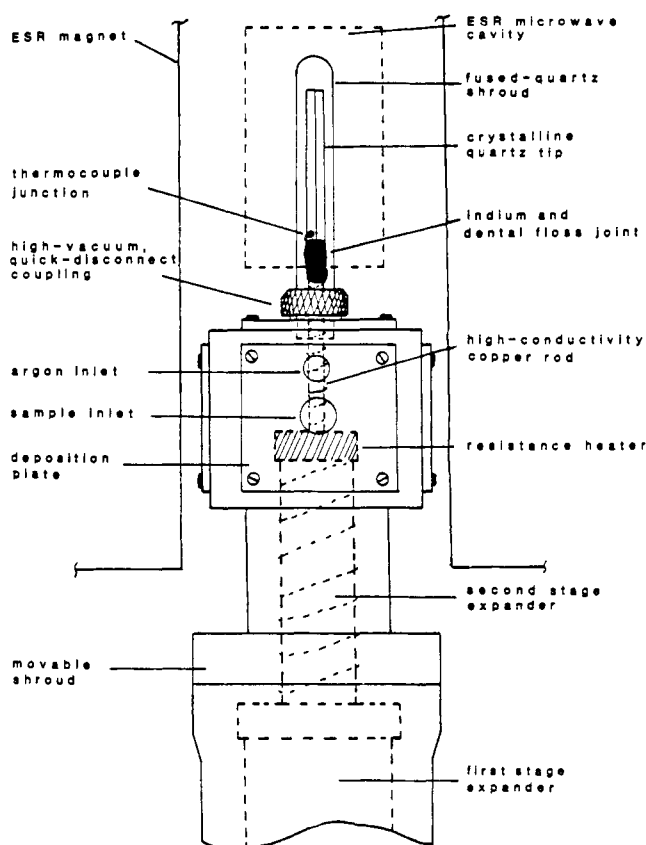


Figure 9. Apparatus for electron spin resonance, matrix-isolation spectroscopy.

shroud by 0.125 in. diameter flexible 321 stainless-steel tubing (Cajon).

**Matrix-Isolation Electron Spin Resonance Spectroscopy.** The apparatus for matrix isolation ESR spectroscopy<sup>59</sup> utilizes an Air Products Model 202 "Displex" cryogenic refrigeration system (Figure 9). The vacuum system and gas handling system are similar to those described previously.<sup>54,59-61</sup> They are mounted on a moveable cart and connected to the cold head by flexible stainless-steel tubing. A square crystalline quartz rod (ca.  $6 \times 0.3 \times 0.3$  cm; obtained from the UCLA Earth and Space Sciences Department, Thin Section Laboratory) serves as the matrix support. The slightly tapered end of the rod is coated with a thin layer of a Pd-Ag paste (Micro-Lok Conductive coating No. 9601; generously supplied by Electro-Science Laboratories, Inc., Pennsauken, NJ) which is fired on the tip at  $900^\circ\text{C}$  to provide a surface which can be soldered. The tip is inserted 0.5 cm into the hollowed-out end of a  $6 \times 0.3$  cm copper rod with indium solder and indalloy flux No. 2 (Indium Corp. of America). The other end of the copper rod is a threaded flange, so the entire tip assembly can be connected to the cold end of the Displex refrigerator with an indium gasket. A gold-chromel thermocouple is secured on the quartz surface just above the solder joint with Cry-con grease (Air Products Co.), covered by an indium sheet, and secured with dental floss. This arrangement provides excellent thermal conductivity between the copper rod and the quartz tip. Experiments show that the extreme end of the quartz tip can cool to 10 K.

The vacuum shroud around the cold tip assembly (Air Products Model DMX-1A/15) offers 3 in. of vertical movement. This movement allows formation of a matrix on the quartz tip from the same deposition plate used with the infrared apparatus. After the deposition, the shroud can be lowered vertically to position the quartz tip in a fused quartz extension in the base of the shroud. This allows the matrix to be positioned directly inside the ESR cavity. The sample is irradiated while in the cavity. The magnet and microwave bridge are turned off during the irradiation. Sample irradiation is discontinued while spectra are being recorded.

**Sample Deposition.** Sufficiently volatile samples which are stable in the vapor phase at room temperature can be introduced directly into the

(59) Kreil, C. L. Ph.D. Dissertation, University of California, Los Angeles, CA, 1983.

(60) Sheridan, R. S. Ph.D. Dissertation, University of California, Los Angeles, CA, 1979.

(61) West, P. R. Ph.D. Dissertation, University of California, Los Angeles, CA, 1980.

gas handling system. After dilution with the matrix gas (typically 99.999% Ar) to a ratio between 1/500 and 1/1000, the sample can be deposited by either the pulsed-deposition method or the slow-spray method described elsewhere.<sup>54,59</sup>

Nonvolatile samples, and samples which are unstable in the vapor phase at room temperature, require the direct-deposition method. In these cases, pure argon is deposited onto the window from the gas handling system, and the sample is sublimed onto the window simultaneously via a separate line in the deposition plate. The appropriate sublimation rate is determined empirically, by varying the temperature of the sample. Sample and argon mixing occurs just before reaching the cold surface. The argon flow is monitored by the differential pressure gauge and adjusted so the pressure change is 0.25 to 1.0 mm min<sup>-1</sup> for the 3-L ballast. The rate of sample deposition is varied to yield well-isolated material, as judged by the degree of spectral resolution. Generally, truly isolated species exhibit bandwidths in the infrared of less than 1 cm<sup>-1</sup> at half-height. For infrared studies, generally 50–200 mm of argon (or argon-sample) are deposited. For UV-vis spectroscopy, the sample amount required is much less. The relative amount depends largely on the extinction coefficient of the sample. Sample is deposited until the maximum absorbance is ca. 2–3, requiring about one-tenth the deposition time for an infrared experiment. The sample-to-argon ratio is maintained constant, so only 5–25 mm of argon is deposited.

The window temperature is critical for the degree of matrix isolation in the experiment. Usually 25–28 K is optimum for deposition of argon. Above this range the argon softens and the substrate diffuses through the matrix, resulting in aggregation and loss of spectral resolution. Lower temperatures lead to a crystalline matrix, producing severe light scattering.

**Irradiation Techniques.** Irradiations were carried out by an ILC Technology LX300UV 300W high-pressure xenon arc lamp with an Electronic Measurements, Inc. Model ELXE-500A power supply. A 10-cm path length of distilled water served as an infrared filter to minimize heating of the matrix during irradiation. Wavelength control was provided by either glass cutoff glass filters (<0.1% transmittance of wavelengths shorter than the specified values) or a Kratos GM252-20, high-intensity, quarter-meter grating monochromator (16-nm band-pass centered at the specified value).

**Layering Experiments.** A photoproduct which absorbs very strongly at the wavelength of irradiation serves as an internal filter over the surface of the matrix, shielding the unreacted starting material deeper in the matrix from light. As a result, only low conversions of starting material are attainable. In order to circumvent this problem, a thin layer of sample and argon is deposited (ca. 10–15% of the usual amount). The matrix is then irradiated until spectra show that the starting material is totally destroyed. This can be accomplished because the matrix is so thin that internal filtering effects are not a problem. The process is then repeated until enough layers have been deposited to obtain a good spectrum of the photoproduct.

**Flash Vacuum Thermolysis/Matrix-Isolation Trapping.** The sample is allowed to sublime through a 10-cm, unpacked, quartz tube wrapped with 18–22 gauge Nichrome wire. An iron vs. Constantan thermocouple is secured with glass tape midway along the length of the tube, and the whole oven is wrapped with asbestos tape. Oven temperature is regulated by two Variac transformers connected in series. This simple setup proved quite reliable and could attain temperature in excess of 900 °C. The pyrolysate co-condenses with argon onto a 15–25 K sample window using standard matrix-isolation sample deposition techniques.

**Acenaphthylene-1,2-dione Mono-*p*-toluenesulfonylhydrazide.**<sup>62</sup> *p*-Toluenesulfonylhydrazide (10.1 g, 0.06 mol; Aldrich, recrystallized from water) was added to a suspension of acenaphthylene-1,2-dione (10.0 g, 0.06 mol; Aldrich) in 100 mL of refluxing methanol. The suspension was refluxed for 24 h and allowed to cool. The resulting solid was recrystallized from a methanol–2-propanol mixture to give the monotosylhydrazide as orange leaflets (14.4 g, 67%): mp 176–177 °C dec (lit. mp 179 °C); <sup>1</sup>H NMR (CDCl<sub>3</sub>) δ 7.90 (m, 10 H), 2.40 (s, 3 H); IR (KBr) 3460 (br), 1695 (vs), 1390 (s), 1360 (s), 1170 (vs), and 395 (vs) cm<sup>-1</sup>.

**2-Diazo-1(2*H*)-acenaphthyleneone (1).**<sup>62</sup> Aqueous sodium hydroxide (40.0 mL, 0.1 N) was added to a solution of acenaphthylene-1,2-dione monotosylhydrazide (3.5 g, 0.01 mol) in 50 mL of dichloromethane. The resulting two-phase system was vigorously stirred for 3 h, and the layers were separated. The organic phase was washed with water, dried over anhydrous sodium sulfate, filtered, and concentrated to 15 mL under reduced pressure. The orange solution was placed on an alumina column and eluted with a 1:1 mixture of pentane and dichloromethane to give 2-diazo-1(2*H*)-acenaphthyleneone as an orange solid (1.3 g, 65%): mp 92–94 °C (lit. mp 92–94 °C); <sup>1</sup>H NMR (CCl<sub>4</sub>) δ 8.10–7.20 (m); IR

(KBr) 2080 (vs), 1680 (vs), 1390 (m), 1330 (m), 1260 (m), 1170 (m), 1100 (m), 1060 (m), 875 (m), 812 (s), and 762 (vs) cm<sup>-1</sup>; UV (cyclohexane) λ<sub>max</sub> 272, 284, 297, 309, 325, 342, and 386 nm. The sample was sublimed at 45 °C (10<sup>-6</sup> torr) and codeposited with argon to form a matrix.

**5,6-Dihydrocyclopent[*fg*]acenaphthylene-1,2-dione Mono-*p*-toluenesulfonylhydrazide.** A stirred suspension of 5,6-dihydrocyclopent[*fg*]acenaphthylene-1,2-dione<sup>63</sup> (1.0 g, 4.81 mmol recrystallized from DMF) and *p*-toluenesulfonylhydrazide (0.895 g, 4.81 mmol; Aldrich, recrystallized from water) in absolute ethanol (100 mL) was slowly warmed to reflux under an atmosphere of nitrogen. After refluxing for 24 h the orange-yellow suspension was cooled to room temperature and the solvent was removed in vacuo. The remaining residue was purified by column chromatography (200 g silica gel, CH<sub>2</sub>Cl<sub>2</sub>) to give the tosylhydrazide as a fluffy yellow solid (0.70 g, 38.7%): mp 220 °C dec (starts to darken at 160 °C); IR (KBr) 1689, 1669, 1614, 1593, 1555, 1539, 1434, 1388, 1352, 1338, 1270, 1226, 1185, 1162, 1117, 1085, 1048, 994, 971, 893, 868, 848, 813, 772, 704, 656, 622, 594, 553, 501, 480, and 414 cm<sup>-1</sup>; UV (95% EtOH) λ<sub>max</sub> 390, 380, 313, and 230 nm; <sup>1</sup>H NMR δ (Me<sub>2</sub>SO-*d*<sub>6</sub>) 8.22–7.37 (m, 4 H), 3.78–3.30 (m, 4 H), and 2.50 (s, 3 H). Further elution recovered starting material, (0.53 g). The yield of tosylhydrazide based on starting material consumed was 82%.

**2-Diazo-5,6-dihydrocyclopent[*fg*]acenaphthylene-1-one (2).** To a stirred suspension of 5,6-dihydrocyclopent[*fg*]acenaphthylene-1,2-dione mono-*p*-toluenesulfonylhydrazide (1.0 g, 2.66 mmol) in 150 mL of dichloromethane was added 40 mL of 0.1 N aqueous sodium hydroxide solution, with the reaction mixture protected from room light. After stirring for 5 h at room temperature, the orange-yellow suspension was placed in a separatory funnel, and the layers were separated. The aqueous layer was extracted twice with 50 mL of dichloromethane, and the organic layers were combined. After drying over sodium sulfate, the solvent was removed in vacuo and the remaining residue purified by column chromatography (neutral alumina, CH<sub>3</sub>CN) to give α-diazo ketone **2** as the first yellow band. After in vacuo removal of the solvent, **2** was obtained as yellow-orange crystals (350 mg, 60%): mp 159.5–161 °C dec (resolidified to a dark brown solid, mp >235 °C); IR (KBr) 2069, 1689, 1664, 1613, 1485, 1464, 1435, 1413, 1369, 1333, 1253, 1223, 1203, 1133, 1044, 998, 938, 847, 825, 814, 758, 718, 617, 506, 483, and 414 cm<sup>-1</sup>; UV (95% EtOH) λ<sub>max</sub> 400, 338, 316, 305, 279, and 270 nm; <sup>1</sup>H NMR (CDCl<sub>3</sub>) δ 7.98–7.24 (m, 1 H) and 3.51 (s, 1 H); high-resolution mass spectrum, calcd for C<sub>14</sub>H<sub>8</sub>N<sub>2</sub>O 220.0636, found 220.0628. The sample was sublimed at 85 °C (10<sup>-6</sup> torr) and codeposited with argon to form a matrix.

**Cyclopent[*fg*]acenaphthylene-1,2-dione Mono-*p*-toluenesulfonylhydrazide.** A stirred suspension of cyclopent[*fg*]acenaphthylene-1,2-dione<sup>63</sup> (2.33 g, 11.3 mmol) and *p*-toluenesulfonylhydrazide (2.11 g, 11.3 mmol; Aldrich, recrystallized from water) in 200 mL of absolute ethanol was slowly warmed to reflux under a nitrogen atmosphere. After 20 h at reflux, the orange-brown suspension was cooled, and the solvent removed in vacuo. The remaining orange-brown solid was recrystallized from a large amount of boiling absolute ethanol to give the tosylhydrazide as fluffy orange-yellow crystals (3.10 g, 73%): mp 155–165 °C dec; IR (KBr) 1727, 1684, 1643, 1635, 1614, 1593, 1573, 1554, 1539, 1518, 1504, 1492, 1463, 1453, 1443, 1393, 1369, 1342, 1297, 1260, 1229, 1183, 1166, 1147, 1118, 1087, 1037, 968, 909, 879, 838, 814, 707, 671, 660, 636, 601, 574, 557, 542, 512, 484, 448, 437, 410, 392, 368, 346, and 316 cm<sup>-1</sup>; UV (95% EtOH) λ<sub>max</sub> 380, 355, 326, and 228 nm; <sup>1</sup>H NMR (Me<sub>2</sub>SO-*d*<sub>6</sub>) δ 8.4–7.2 (m, 10 H) and 2.5 (s, 3 H).

**2-Diazocyclopent[*fg*]acenaphthalene-1-one (3).** To a stirred suspension of cyclopent[*fg*]acenaphthalene-1,2-dione mono-*p*-toluenesulfonylhydrazide (0.5 g, 1.34 mmol) in 50 mL of dichloromethane was added 20 mL of 0.1 N aqueous sodium hydroxide solution, with the reaction mixture protected from room light. After being stirred for 3 h, the dark reaction mixture was placed in a separatory funnel, and the layers were separated. The aqueous layer was extracted three times with 25 mL dichloromethane, and the combined organic extracts were washed with water and brine and dried over sodium sulfate. The solvent was removed in vacuo to give dark crystals of the α-diazo ketone **3** (160 mg, 55%): IR (KBr) 2074, 1725, 1690, 1669, 1644, 1634, 1614, 1555, 1539, 1521, 1505, 1459, 1439, 1409, 1371, 1348, 1259, 1244, 1217, 1122, 1091, 1079, 1021, 992, 952, 934, 822, 717, 665, 640, 590, 560, 510, 495, 481, 371, 346, and 320 cm<sup>-1</sup>; UV (95% EtOH) λ<sub>max</sub> 412, 390, 360, 326, 284, and 234 nm; <sup>1</sup>H NMR (Me<sub>2</sub>SO-*d*<sub>6</sub>) δ 8.4–6.9 (m); high-resolution mass spectrum, calcd for C<sub>14</sub>H<sub>8</sub>N<sub>2</sub>O 218.0480, found 218.0476. The sample was sublimed at 73 °C (10<sup>-6</sup> torr) and codeposited with argon to form a matrix.

**1-Diazocyclopent[*cd*]azulene-2-one (4).** A stirred solution of 364 mg (2.0 mmol) of cyclopent[*cd*]azulene-1,2-dione<sup>32</sup> and 372 mg (2.0 mmol) of *p*-toluenesulfonylhydrazide (Aldrich; recrystallized from water) in 50

(62) Cava, M. P.; Little, R. L.; Napier, D. R. *J. Am. Chem. Soc.* **1958**, *80*, 2257–2263.

(63) Trost, B. M. *J. Am. Chem. Soc.* **1969**, *91*, 918–923.

mL of absolute ethanol was slowly warmed to reflux under an atmosphere of nitrogen. After 1 h the violet solution became orange; the mixture was cooled, and the solvent was removed in vacuo. The remaining orange oil was dissolved in 50 mL of  $\text{CH}_2\text{Cl}_2$ , washed with 50 mL of 2 N NaOH and water, and dried with sodium sulfate. The solvent was removed, and the residue was purified by chromatography on  $\text{Al}_2\text{O}_3$  BIII (Brockmann) with  $\text{CH}_2\text{Cl}_2$ . The first orange fraction was collected. After removal of the solvent in vacuo, the orange residue was twice recrystallized from ethanol to give 234 mg (61%) of 1-diazocyclopent[cd]azulene-2-one (**4**) as dark brown needles: mp 115 °C; IR (KBr) 2061, 1715, 1695, 1668, 1652, 1596, 1568, 1538, 1520, 1506, 1455, 1446, 1425, 1375, 1313, 1261, 1229, 1153, 1031, 847, 790, 750, 731, 635, 588, and 422  $\text{cm}^{-1}$ ; UV (Ar-Matrix)  $\lambda_{\text{max}}$  435, 422, 408, 397, 385, 354, 337, 320, 302, 279, 267, 239, and 230 nm;  $^1\text{H}$  NMR ( $\text{CDCl}_3$ )  $\delta$  8.4–7.3 (m); high-resolution mass spectrum; calcd for  $\text{C}_{12}\text{H}_6\text{N}_2\text{O}$  194.0481, found 194.0476. The sample was sublimed at 80 °C ( $10^{-6}$  torr) and codeposited with argon to form a matrix.

**1,2,3-H-2-Diazophenalene-1,3-dione (15).** The diazodione was prepared by the method of Regitz<sup>64</sup> and gave analytical data as reported. The sample was sublimed at 91 °C ( $10^{-6}$  torr) and codeposited with argon to form a matrix.

**1,2-Dihydroacenaphthylene-5,6-dicarboxylic Anhydride (16).** The anhydride was prepared by the method of Carpino and Gowecke<sup>29</sup> as modified by Trost.<sup>30</sup> The infrared spectrum of **16** could not be obtained under argon-matrix isolation conditions due to the low volatility of the sample.

**Acenaphthylene-5,6-dicarboxylic Anhydride (18).** A stirred suspension of dimethyl acenaphthylene-5,6-dicarboxylate<sup>29</sup> (5.0 g, 18.7 mmol) in 100 mL of 60% aqueous sulfuric acid was warmed to reflux. After 45 min, the red-orange suspension was cooled to room temperature and vacuum-filtered through a glass-fritted funnel to give anhydride **18** as an

orange-red solid (4.05 g, 98%): mp >230 °C; IR (KBr) 2913, 2849, 1774, 1765, 1735, 1710, 1690, 1649, 1624, 1569, 1559, 1548, 1539, 1519, 1501, 1489, 1458, 1443, 1409, 1369, 1348, 1298, 1262, 1227, 1213, 1200, 1152, 1128, 1099, 1050, 987, 959, 857, 807, 749, 734, 694, 669, 644, 498, 411, 361, 350, and 319  $\text{cm}^{-1}$ ; UV (95% EtOH)  $\lambda_{\text{max}}$  360 and 240 nm; high-resolution mass spectrum, calcd for  $\text{C}_{14}\text{H}_6\text{O}_3$  222.0317, found 222.0326. The infrared spectrum of **18** could not be obtained under argon-matrix isolation conditions due to the low volatility of the sample.

**Acknowledgment.** This research was supported by Grant CHE81-11196 from the National Science Foundation and by a grant from the International Business Machine Corporation. We are grateful to Dr. Curtis Kreil for technical assistance with the matrix isolation ESR apparatus and Professor Klaus Hafner for a sample of cyclopent[cd]azulene-2-one (**21**). Predoctoral fellowships (R.J.M.) were provided by the National Science Foundation (1980–1983) and the International Business Machine Corporation (1983–1984). H.P.K. is a Feodor Lynen Postdoctoral Fellow of the Alexander von Humboldt Foundation.

**Registry No.** **1**, 2008-77-7; **2**, 87985-99-7; **3**, 87986-00-3; **4**, 98361-78-5; **5**, 98361-79-6; **6**, 98361-80-9; **8**, 98361-81-0; **9**, 82515-17-1; **10**, 86998-10-9; **11**, 87016-12-4; **12**, 98361-82-1; **13**, 81-84-5; **14**, 98361-83-2; **15**, 18931-19-6; **16**, 5699-00-3; **17**, 98361-84-3; **18**, 21973-76-2; **19**, 98361-85-4; **20**, 98361-86-5; **21**, 52711-37-2; acenaphthylene-1,2-dione, 82-86-0; *p*-toluenesulfonyl hydrazide, 1576-35-8; acenaphthylene-1,2-dione mono-*p*-toluenesulfonylhydrazone, 66365-89-7; 5,6-dihydrocyclopent[fg]acenaphthylene-1,2-dione, 5254-01-3; 5,6-dihydrocyclopent[fg]acenaphthylene-1,2-dione mono-*p*-toluenesulfonylhydrazone, 98361-87-6; cyclopent[fg]acenaphthylene-1,2-dione, 5253-87-2; cyclopent[fg]-acenaphthylene-1,2-dione mono-*p*-toluenesulfonylhydrazone, 98361-87-6; cyclopent[cd]azulene-1,2-dione, 52711-38-3; dimethyl acenaphthylene-5,6-dicarboxylate, 92964-95-9.

(64) Regitz, M. *Liebigs Ann. Chem.* **1964**, 676, 101–109.

## Mechanism of the Chromium-Catalyzed Epoxidation of Olefins. Role of Oxochromium(V) Cations

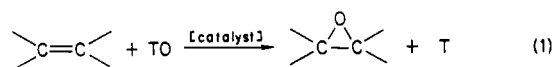
E. G. Samsel, K. Srinivasan, and J. K. Kochi\*

Contribution from the Chemistry Department, University of Houston, University Park, Houston, Texas 77004. Received April 29, 1985

**Abstract:** The catalytic epoxidation of various olefins with iodobenzene is efficiently carried out by a series of chromium(III) cations  $\text{Cr}^{\text{III}}(\text{salen})^+$  (I) which are promoted by pyridine *N*-oxide (pyO) and related oxygen donors as the cocatalyst. Analysis of the catalytic rate profile and products establish the oxochromium(V) derivative  $\text{O}=\text{Cr}(\text{salen})^+$  (II) and its donor adduct  $\text{O}=\text{Cr}(\text{salen})(\text{pyO})^+$  (III) as the reactive intermediates in the catalytic cycle. The successful isolation as well as the complete spectral analysis and structural characterization by X-ray crystallography of both II and III reveal the basis for oxygen activation in the  $\text{O}=\text{Cr}^{\text{V}}$  functionality. The mechanism of oxygen atom transfer involves the rate-limiting attack on the olefin by the electrophilic oxochromium(V) cation. The observation of benzaldehyde as a byproduct derived from the pyO-promoted C=C cleavage of styrene provides a method for unequivocally proving the existence of a transient intermediate during oxygen atom transfer. Thus the rate of olefin oxidation is found to be completely independent of the product-forming steps leading to epoxide and benzaldehyde, as they are modulated by added pyO. Steric effects, isotopic  $^{18}\text{O}$  tracers, stereochemistry, skeletal rearrangement, and substituent effects all provide mechanistic probes for the structure of the metastable intermediate.

The catalytic functionalization of various types of hydrocarbons with such terminal oxidants (TO) as dioxygen, peroxides, nonmetal oxides, etc., is of both chemical and biochemical importance.<sup>1</sup> Among such transformations, the metal-catalyzed conversion of an olefin to its epoxide by oxygen atom transfer poses an intriguing synthetic as well as theoretical challenge.<sup>2</sup> In this regard Groves

and co-workers have introduced the interesting notion of oxygen rebound, in which the oxygen atom is successively transferred from the terminal oxidant to the metal catalyst and thence to the olefin.<sup>3</sup> Accordingly, a crucial role is played by a reactive oxometal intermediate for which there is recent experimental support.<sup>4</sup>



(1) For a review, see: Sheldon, R. A.; Kochi, J. K. "Metal-Catalyzed Oxidations of Organic Compounds"; Academic: New York 1981.

(2) See: Berti, G. "Topics in Stereochemistry"; Allinger, N. L., Eliel, E. L. Eds.; Wiley: New York, 1973; Vol. V. Rappe, A. K.; Goddard, W. A., III *J. Am. Chem. Soc.* **1982**, 104, 3287.

(3) (a) Groves, J. T.; McClusky, G. A. *J. Am. Chem. Soc.* **1976**, 98, 859. (b) Groves, J. T.; Nemo, T. E.; Myers, R. S. *J. Am. Chem. Soc.* **1979**, 101, 1032. (c) See also: Guengerich, F. P.; McDonald, T. L. *Acc. Chem. Res.* **1984**, 17, 9.